NMR Metabolomics to Revisit the Tobacco Mosaic Virus Infection in *Nicotiana tabacum* Leaves

Young Hae Choi,[†] Hye Kyong Kim,[†] Huub J. M. Linthorst,[‡] Johan G. Hollander,[§] Alfons W. M. Lefeber,[§] Cornelis Erkelens,[§] Jean-Marc Nuzillard,[⊥] and Robert Verpoorte*[,†]

Division of Pharmacognosy, Section Metabolomics, Institute of Biology, Leiden University, P.O. Box 9502, 2300 RA Leiden, The Netherlands, Division of Plant Cell Physiology, Institute of Biology, Leiden University, P.O. Box 9502, 2300 RA Leiden, The Netherlands, Division of NMR, Institute of Chemistry, Gorlaeus Laboratories, P.O. Box 9502, 2300 RA Leiden, The Netherlands, and Laboratoire de Pharmacognosie, FRE CNRS 2715, IFR 53 Biomolecules, CPCBAI, B.P. 1039, Moulin de la Housse, 51687 Reims Cedex, France

Received December 18, 2005

Tobacco mosaic virus (TMV) infection of tobacco is a well-known and extensively studied model system for which a number of genes and proteins involved in the systemic acquired resistance (SAR) have been characterized. Little is known about the metabolic changes connected with the infection and SAR. Here we describe the use of NMR spectroscopy in combination with multivariate data analysis to study the metabolic changes. Particularly 2-D NMR methods, such as 2-D *J*-resolved spectra and their projected spectra, are shown to be powerful tools in the metabolomic studies. The macroscopic view of the metabolomes obtained by NMR spectroscopy of crude extracts enabled the identification of a series of totally different metabolites that seem connected with resistance, such as the clearly increased 5-caffeoylquinic acid, α-linolenic acid analogues, and sesqui- and diterpenoids in the infected plant parts.

Genes are the blueprint of the cell factory and encode the production of the enzymes and metabolites involved in the defense against pests and diseases. One of the most extensively studied systems for plant defense against viral diseases is the tobacco mosaic virus (TMV) infection of tobacco. Characteristic for this defense is the systemic acquired resistance (SAR). After infection of a leaf with TMV, this leaf will signal other leaves to express the genes involved in SAR, which makes these leaves resistant against the virus. Despite the importance of metabolites involved in this defense system, most studies have been performed only at the level of the genes and the proteins.[1,2] However, little is known about the metabolic changes connected to SAR,[3−5] and no total metabolomic analysis has been performed on SAR.

To study the total metabolomic changes, several technology platforms are being developed. Some are based on chromatography (e.g., GC-MS and LC-MS) and others on MS spectrometry or NMR spectroscopy. None of these are capable of achieving the ultimate goal of analyzing all metabolites in an organism both qualitatively and quantitatively. First of all it is because of the enormous number of compounds involved and the large differences in amounts and in the physical characteristics of the compounds. In addition, some methods have inherent limitations as metabolomic tools. For instance, chromatography and MS suffer from problems of reproducibility and require calibration curves for all individual compounds for an absolute quantitation. NMR spectroscopy scores much better for this: the signal intensity for all compounds is dependent only on the molar concentration, and reproducibility is very high. The disadvantage if compared with the other methods is that it requires more material, as it is less sensitive. However, due to the mentioned advantages, NMR has developed into a major tool for the analysis of body fluids such as urine (metabonomics), e.g., for the identification of biomarkers for diseases.[6−8]

An increasing number of studies concerning plant NMR metabolomics are being reported, although no international standardization has been achieved yet and maybe is not even of high priority because of the high reproducibility of NMR. Here we report the use of NMR spectroscopy in combination with multivariate data analysis to, in a macroscopic way, determine the metabolic changes in tobacco plants infected with TMV.

Results and Discussion

The first step of a metabolomics study is a qualitative analysis of the spectra of the plant extracts. In a previous publication on the NMR metabolomics of transgenic tobacco plants overexpressing salicylate biosynthetic genes, we identified a number of compounds.[9] However, due to overlap of signals, most of them remained unidentified. To overcome the problem of the congestion of 1-D ^{1}H NMR spectra, several kinds of 2-D NMR methods were evaluated for the plant extracts. Among the 2-D NMR techniques evaluated, the 2-D *J*-resolved NMR technique greatly improved the resolution of the ^{1}H NMR spectra and it may facilitate identification of metabolites from extracts (Figure 1a). The congested signals around δ 6.4 were clearly separated and proved to be three *trans* H-8′ olefinic protons bearing the same coupling constants ($J = 15.9$ Hz), typical for cinnamate derivatives. Isolation by column chromatography followed by 2-D NMR spectroscopy analysis including COSY, HSQC, and HMBC led to their identification as three isomers of caffeoylquinic acid: 3-*O*-, 4-*O*-, and 5-*O*-caffeoylquinic acid. In addition, using the *J*-resolved spectra, the complex signals of citric acid, malic acid, succinic acid (Figure 1b), and cembratriene analogues (signals clustered at δ 1.30−1.70) (Figure 1c) were identified. The chemical shifts and the structures of the metabolites of tobacco leaves detected in the ^{1}H NMR spectra are listed in Table 1 and Figure 2, respectively.

By projecting the *J*-resolved spectrum on the chemical shift axis all protons ideally appear as a singlet similar to ^{13}C NMR spectra, showing a fully H-decoupled spectrum. This projected spectrum greatly enhances resolution and circumvents the problem of second-order effects connected with different field strengths.[10] The degree of complexity in the projected *J*-resolved spectrum is significantly reduced compared with the raw ^{1}H NMR data set and has a major advantage in that the shifts of the signals are independent of the field strength (Figure 3).

After qualitative analysis the quantitative phase starts by comparing the spectra of many samples of plants treated in different ways. We applied the enhanced resolution from the projected *J*-resolved spectra to monitor metabolic changes in the leaves of healthy and TMV-infected plants measured 1, 3, 7, and 10 days after infection. For the analysis of the large data sets, principal component analysis (PCA) was used to reduce the numerous NMR signals of the plant

* Corresponding author. Tel: +31-71-527-4528. Fax: +31-71-527-4511. E-mail: verpoort@chem.leidenuniv.nl.
[†] Division of Pharmacognosy, Leiden University.
[‡] Division of Plant Cell Physiology, Leiden University.
[§] Division of NMR, Leiden University.
[⊥] Laboratoire de Pharmacognosie, Reims University.

10.1021/np050535b CCC: $33.50
Published on Web 04/20/2006

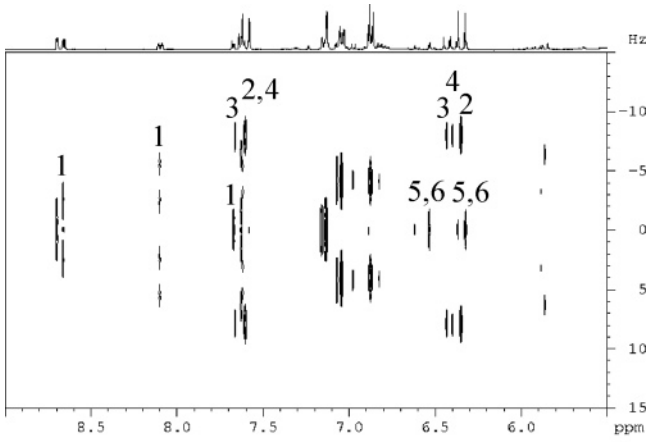

a

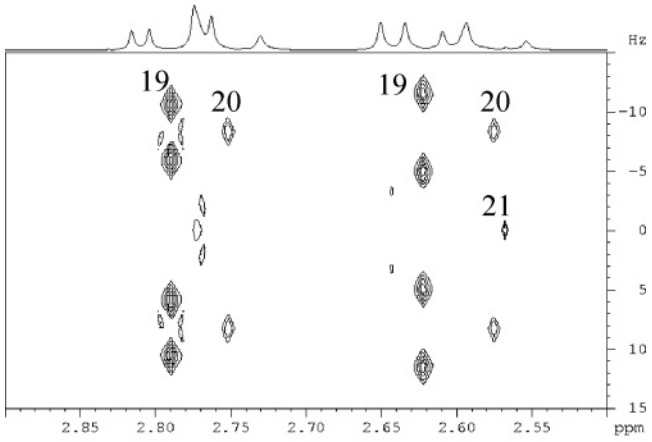

b

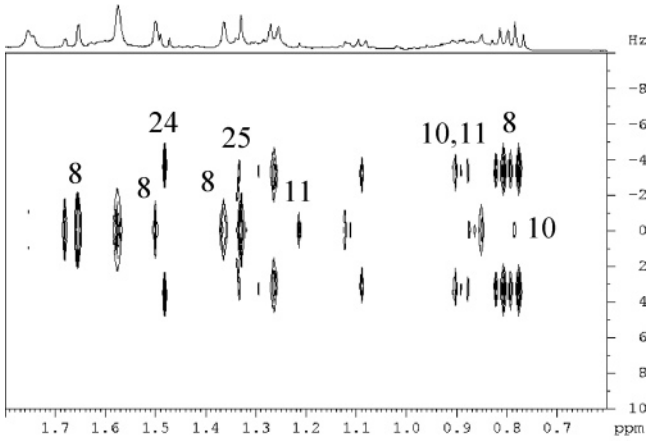

c

Figure 1. 2-D *J*-resolved NMR spectra of healthy *N. tabacum* leaves in the range δ 5.5−9.0 (a), δ 2.4−3.0 (b), and δ 0.6−1.8 (c). Numbering of signals follows the system of Table 1. For details of assignments of the signals, see Table 1. (1) nicotine, (2) 3-*O*-caffeoylquinic acid, (3) 4-*O*-caffeoylquinic acid, (4) 5-*O*-caffeoylquinic acid, (5) quercetin, (6) kaempferol, (8) cembranoids, (10) steroids, (11) fatty acids, (19) malic acid, (20) citric acid, (21) succinic acid, (24) alanine, (25) threonine.

extracts to one or two principal components that are characteristic for the metabolic changes after TMV infection. The score plots for PC1 versus PC2 from the projected *J*-resolved spectra show

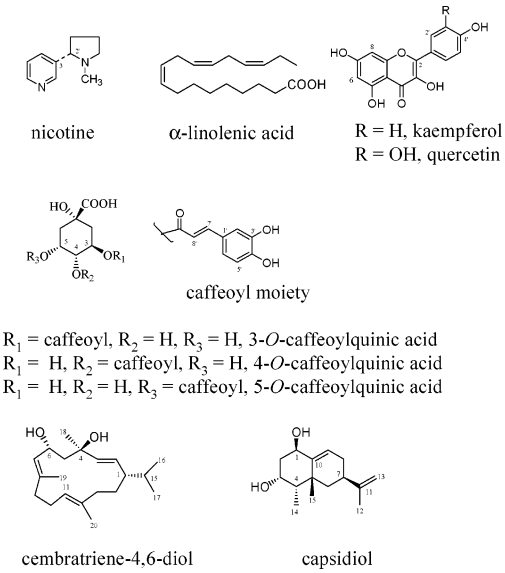

Figure 2. Chemical structures of some metabolites identified in the NMR spectra of *N. tabacum* leaves.

that the leaves of infected tobacco are clearly separated from healthy ones (Figure 4a), for both the locally infected and systemic acquired resistance (SAR) leaves. The separation is mainly due to PC1. However, aging of the leaves during the experiment also shows a shift along the PC1 axis. To exclude differences due to biological variability, PCA was performed only on the control and the TMV locally infected leaves of the same developmental stage. This gives quite a pronounced separation (Figure 4b).

The local infection is mainly characterized by PC3, in which phenylpropanoids (e.g., 3-*O*-, 4-*O*-, and 5-*O*-caffeoylquinic acid), quercetin, sucrose, glucose, inositol, alanine, glutamine, proline, and α-linolenic acid analogues were found to be the major contributing metabolites by analysis of a loading plot. Intriguingly, among the phenylpropanoids, only 5-*O*-caffeoylquinic acid accumulates more in the locally infected leaves. Phenylpropanoids including 3-*O*-caffeoylquinic acid (chlorogenic acid) serve as phytoanticipins in many plant species.[11] Tobacco plants overexpressing L-phenylalanine ammonia lyase (PAL), the entry point enzyme into the phenylpropanoid pathway, produce high levels of chlorogenic acid and exhibit a markedly reduced susceptibility to infection with the fungal pathogen *Cerospora nicotianae*.[12] Reduction of phenylpropanoid biosynthesis in tobacco by down-regulation of PAL seriously compromises both local resistance and systemic acquired resistance to viral infection.[13] However, it remains unclear which phenylpropanoid analogues confer resistance in wild-type tobacco. The 5-*O*-caffeoylquinic acid in the infected local leaves increased gradually through the whole experimental period (10 days) after TMV inoculation, whereas the level of the other two isomers declined. On the basis of these results, it can be postulated that 5-*O*-caffeoylquinic acid might be involved in the defense mechanism against TMV infection.

In the locally infected leaves there was a considerable decrease in the level of a metabolite having signals at δ 3.60, 3.44, and 3.24. Using TOCSY and HMBC, those signals were identified to be H-4 and H-6, H-1 and H-3, and H-5 of inositol, respectively. Previously it has been reported that transgenic tobacco expressing *Stpd1*, a cDNA-encoding sorbitol-6-phosphate dehydrogenase from apple, under the control of a cauliflower mosaic virus 35S promoter, showed a low level of *myo*-inositol, which correlated with the appearance of lesions.[14] It was thought that the significant decrease of inositol alongside hyperaccumulation of sorbitol, which interferes with inositol biosynthesis, might lead to osmotic imbalance, possibly acting as a signal affecting carbohydrate allocation and transport.[14] Other experiments have been reported on the role of inositol in

Table 1. ^{1}H Chemical Shifts of Metabolites of *N. tabacum* Leaves Detected from 1-D and 2-D NMR Spectra

no.	metabolite	chemical shifts (ppm) and coupling constants (Hz)
1	nicotine	δ 8.70 (H-2, d, J = 2.0 Hz), δ 8.66 (H-6, dd, J = 4.9 Hz, 1.5 Hz), δ 8.10 (H-4, dt, J = 4.9 Hz, 1.5 Hz), δ 2.77 (*N*-methyl, s)
2	3-*O*-caffeoylquinic acid[a]	δ 7.60 (H-7′, d, J = 15.9 Hz), δ 7.15 (H-2′, d, J = 2.1 Hz), δ 7.05 (H-6′, d, J = 8.4 Hz, 2.0 Hz), δ 6.87 (H-5′, d, J = 8.4 Hz), δ 6.36 (H-8′, d, J = 15.9 Hz), δ 5.33 (H-3, td, J = 10.0 Hz, 4.8 Hz), δ 4.21 (H-5, br q, J = 3.1 Hz), δ 3.80 (H-4, dd, J = 9.9 Hz, 3.2 Hz), δ 2.17 (H-2β, H-6β, m), δ 2.04 (H-2α, H-6α, m)
3	4-*O*-caffeoylquinic acid[a]	δ 7.66 (H-7′, d, J = 15.9 Hz), δ 7.17 (H-2′, d, J = 2.0 Hz), δ 7.08 (H-6′, dd, J = 8.4 Hz, 2.0 Hz), δ 6.87 (H-5′, d, J = 8.4 Hz), δ 6.44 (H-8′, d, J = 15.9 Hz), δ 4.89 (H-4, dd, J = 8.4 Hz, 3.0 Hz), δ 4.29 (H-3, br q, J = 3.8 Hz), δ 4.21 (H-5, br q, J = 3.1 Hz), δ 2.17 (H-2β, H-6β, m), δ 2.04 (H-2α, H-6α, m)
4	5-*O*-caffeoylquinic acid*	δ 7.60 (H-7′, d, J = 15.9 Hz), δ 7.14 (H-2′, d, J = 2.0 Hz), δ 7.05 (H-6′, d, J = 8.4 Hz, 2.0 Hz), δ 6.89 (H-5′, d, J = 8.4 Hz), δ 6.41 (H-8′, d, J = 15.9 Hz), δ 5.33 (H-5, td, J = 10.0 Hz, 4.8 Hz), δ 4.09 (H-3, td, J = 10.0 Hz, 4.8 Hz), δ 3.75 (H-4, dd, J = 9.9 Hz, 3.2 Hz), δ 2.17 (H-2β, H-6β, m), δ 2.04 (H-2α, H-6α, m)
5	quercetin	δ 6.99 (H-5′, d, J = 8.6 Hz), δ 6.52 (H-8, d, J = 1.8 Hz), δ 6.28 (H-6, d, J = 1.8 Hz)
6	kaempferol	δ 8.04 (H-2′ and H-6′, d, J = 8.6 Hz), δ 6.74 (H-3′ and H-5′, d, J = 8.6 Hz), δ 6.52 (H-8, d, J = 2.0 Hz), δ 6.28 (H-6, d, J = 2.0 Hz)
7	rhamnose in flavonoid	δ 1.10 (3-*O*-rhamnosylglucoside, H-6, d, J = 6.1 Hz)
8	cembratriene-4,6-diol[a]	δ 0.79 (H-16, d, J = 6.8 Hz), δ 0.81 (H-17, d, J = 6.8 Hz), δ 1.38 (H-18, s), δ 1.52 (H-19, s), δ 1.70 (H-20, s)
9	capsidiol[a]	δ 0.86 (H-14, d, J = 6.8 Hz), δ 1.33 (H-15, s), δ 1.74 (H-12, s), δ 4.33 (H-1, *t*, J = 3.4 Hz), δ 4.51 (H-3, dt, J = 12.4 Hz, 4.5 Hz), δ 4.73 (H-13, d, J = 13.0 Hz), δ 5.96 (H-9, dd, J = 7.0 Hz, 1.8 Hz)
10	steroids	δ 0.78 (H-18, s), δ 0.85 (H-19, s), δ 0.89 (H-21, d, J = 7.0 Hz)
11	fatty acids	δ 0.88 (H-ω, t, J = 7.5 Hz)
12	α-linolenic acids	δ 0.96 (H-ω, t, J = 7.5 Hz), δ 1.30 (CH_2 brs)
13	sucrose	δ 5.40 (H-1, d, J = 3.8 Hz), δ 4.17 (H-1, d, J = 8.5 Hz)
14	α-glucose	δ 5.20 (H-1, d, J = 3.8 Hz)
15	β-glucose	δ 4.59 (H-1, d, J = 7.9 Hz)
16	fructose	δ 4.11 (H-1, d, J = 3.5 Hz)
17	inositol	δ 4.00 (H-2, t, J = 2.8), δ 3.61 (H-4 and 6, t, J = 9.9), δ 3.44 (H-1 and 3, dd, J = 9.9 Hz, 2.9 Hz), δ 3.24 (H-5, t, J = 9.3 Hz)
18	ascorbic acid	δ 4.52 (H-4, d, J = 2.0 Hz)
19	malic acid	δ 4.32 (H-α, dd, J = 6.6 Hz, 4.7 Hz), δ 2.80 (H-β, dd, J = 16.6 Hz, 4.7 Hz), δ 2.61 (H-β', dd, J = 16.6 Hz, 6.6 Hz)
20	citric acid	δ 2.74 (H-β, d, J = 17.6 Hz), δ 2.56 (H- β', d, J = 17.6 Hz)
21	succinic acid	δ 2.54 (s)
22	glutamine	δ 3.72 (H-2, t, J = 6.1 Hz), δ 2.45 (H-3, m)
23	proline	δ 4.08 (H-2, dd, J = 8.6 Hz, 6.4 Hz), δ 2.34 (H-3, m)
24	alanine	δ 1.48 (H-3, d, J = 7.2 Hz)
25	threonine	δ 1.32 (H-5, d, J = 6.6 Hz)

[a] Signals are based on isolated compounds from the experimental plant.

tobacco. The uptake of [^{3}H]- or [^{14}C]-labeled inositol was found to be highly increased in stressed tobacco cells (Wisconsin 38 and Bright yellow 2), and the inositol was incorporated into pectin and phosphoinositides. Inositol in tobacco leaves infected by TMV might thus be involved in the biogenesis of the cell wall, phospholipid signaling pathway, or regulation of cytoskeletal structure.[15−18] The significance of the decrease of inositol in the locally infected tobacco leaves is not yet clear but might be connected with the above-mentioned observations.

The onset of the accumulation of each metabolite was investigated at different stages of the TMV infection. During growth after inoculation, the locally infected leaves extracts show a consistent shift to higher PC1, whereas PC3 separates the infected from healthy leaves (Figure 4b). The projected *J*-resolved NMR signals were quantified for each tobacco sample on different days after inoculation in order to investigate the metabolic changes through time. On the first day after inoculation primary metabolites such as glucose, malic acid, and citric acid significantly increased. On the third day post-inoculation for the infected leaves a definitely different metabolome is observed. The NMR signals corresponding to 5-*O*-caffeoylquinic acid, alanine, glutamine, proline, and α-linolenic acid analogues clearly increased as compared with healthy leaves. On the contrary, sucrose, glucose, inositol, nicotine, malic acid, and 3-*O*- and 4-*O*-caffeoylquinic acid showed a lower level in the infected leaves when compared with healthy plants. Comparison of the 2-D *J*-resolved spectra of healthy and locally infected leaves shows a dramatic accumulation of α-linolenic acid analogues in the infected leaves on the third day (signals at δ 0.96, t, J = 7.5 Hz) (Figure 5). Linolenic acid is the precursor to jasmonate in the octadecanoid cascade. Jasmonate functions as a signal molecule and activates defense-related genes.[19] The accumulation of α-linolenic acid analogues in the locally infected leaves could thus be due to induction of octadecanoid biosynthesis by the TMV infection. However, assuming the α-linolenic acid analogues as signal molecules in the TMV-infected tobacco, the induction time is quite slow (more than 3 days) and the level of concentration is definitely high. These results suggest another possibility; α-linolenic acid analogues might play a direct role in the plant defense instead of as signal molecules. Seven and 10 days after inoculation, the metabolomic changes compared with healthy leaves were similar to those observed at 3 days after inoculation. Therefore it is concluded that the TMV infection initiates a chain of events beginning with the mobilization of glucose, probably as energy source for cells to start up the defense-related metabolism. Subsequently α-linolenic acid and analogues are produced, which might serve as precursors for a defense-inducing signal compound, jasmonate, or play an active role as such in the plant defense. Also

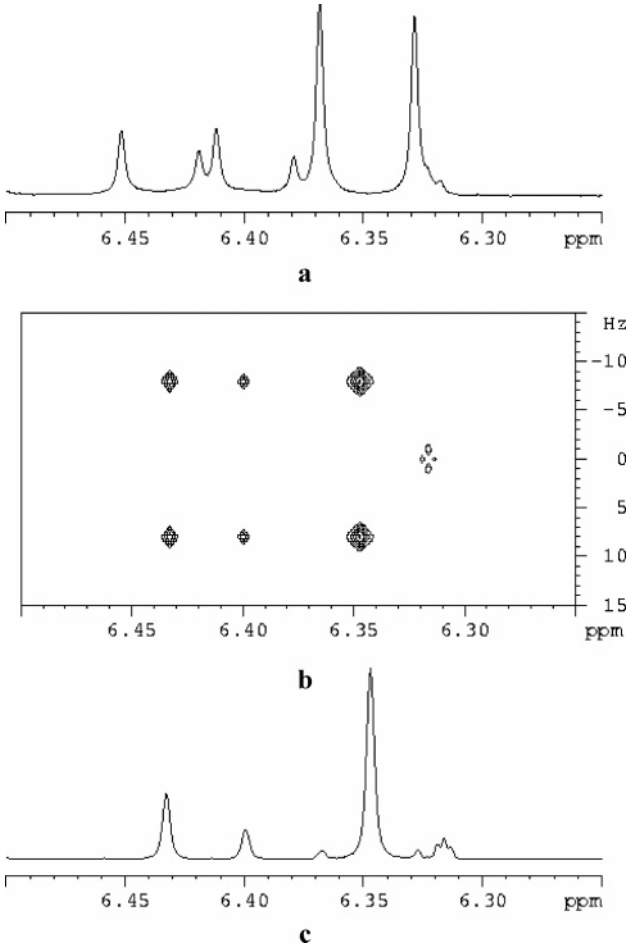

Figure 3. ^{1}H NMR (a), 2-D *J*-resolved (b), and projected 1-D *J*-resolved (c) spectra of healthy *N. tabacum* leaves in the range δ 6.25−6.50.

the caffeoylquinic acid production is altered, which might be related to cell wall modification.

Metabolic alterations of SAR leaves were investigated in a manner analoguos with that for locally infected leaves. It resulted in a clear discrimination between the upper SAR leaves of the TMV-infected plants and those of corresponding healthy leaves (Figure 4c) by PC1. Most of the differentiating metabolites for the PCA separation were the same as for local infection. Phenylpropanoids (e.g., 3-*O*-, 4-*O*-, and 5-*O*-caffeoylquinic acid), sucrose, glucose, malic acid, alanine, glutamine, proline, and α-linolenic acid analogues were found to be altered in the SAR leaves. The decrease of inositol content detected in the SAR leaves was observed only on the 10th day after inoculation.

Apart from these metabolites, several sesquiterpenoids showed a higher accumulation in the SAR leaves. An array of doublets (J = 7.0 Hz) between δ 0.8 and 0.9 was assigned to the characteristic H-14 signals of the eremophylene group of sesquiterpenoids such as capsidiol, debneyol, 5-epiaritolochene, and rishitin.[15] The presence of several eremophylene-type sesquiterpenoids was confirmed by HMBC correlation between H-14 and C-3 at δ 60.0−65.0, C-4 at δ 40.0−43.0, and C-5 at δ 47.0. For a detailed investigation of these metabolites, extracts of healthy upper and SAR leaves were analyzed by gas chromatography using capsidiol as a reference compound. Capsidiol accumulated to more than 2-fold higher levels in the SAR leaves than in healthy ones together with an increase of diterpenoids such as cembratriene-4,6-diol. The higher accumulations of capsidiol, solavetivone, 3-hydroxysolavetivone, 3-hydroxylubumin, rishitin, epirishitin, glutinose, oxyglutinose, solanascone, phytuberin, and phytuberol in *Nicotiana species* leaves after TMV infection or stress have previously been reported.[20−22] However,

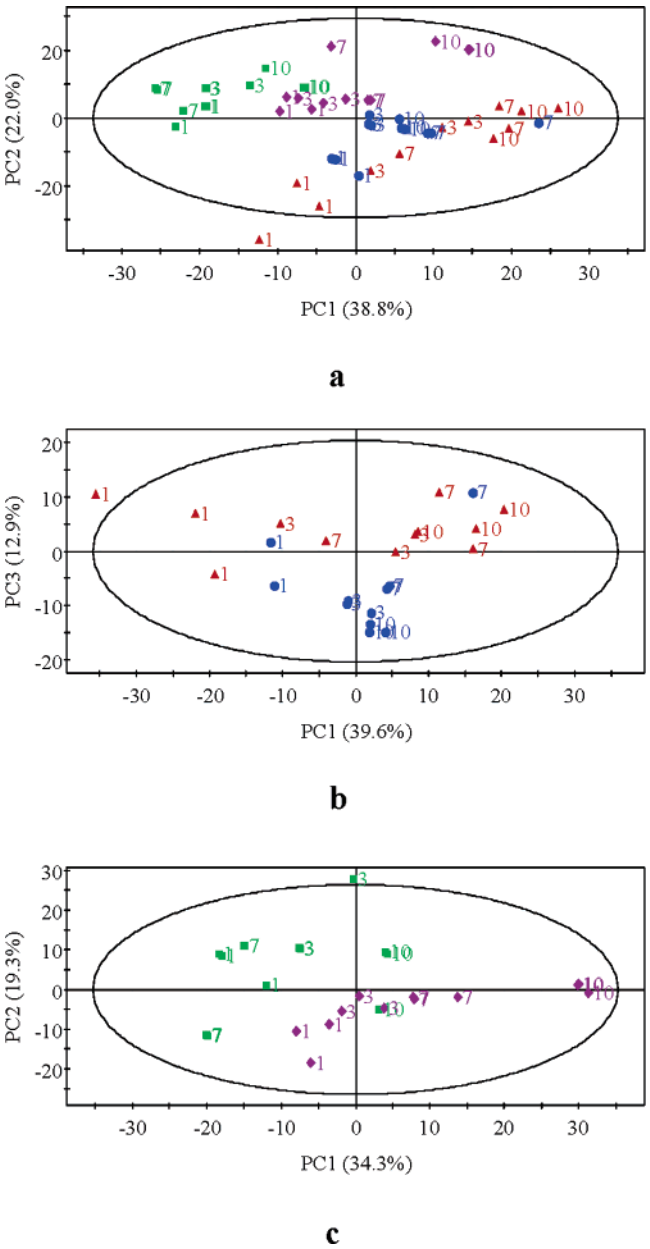

Figure 4. Score plot of principal component analysis of healthy and infected *N. tabacum* leaves by TMV. (●) lower leaves of healthy plants, (■) upper leaves of healthy plants, (▲) locally infected leaves of TMV-infected plants, (◆) systemic acquired resistance leaves of TMV-infected plants. (a) Principal component analysis for lower and upper leaves in healthy plants and inoculated and systemic acquired resistance leaves. (b) PCA for lower leaves in healthy plants and inoculated leaves in the infected plants. (c) PCA for upper leaves in healthy plants and systemic acquired resistance leaves in the infected plants. The ellipse represents the Hotelling T2 with 95% confidence in score plots. Numberings on the plot are the number of days after infection.

there is no change in locally infected leaves when compared with SAR leaves. This indicates that terpenoid biosynthesis is specifically initiated in SAR leaves. Flavonoids (quercetin and kaempferol) are also induced in the SAR leaves.

The comparison of NMR spectra from the SAR leaves and healthy leaves showed that all detected metabolites rapidly decreased in SAR leaves on the first day after inoculation. Alanine reaches its maximum in the SAR leaves on the third day. On the seventh day post-inoculation malic acid and flavonoids accumulated at the highest levels in the SAR leaves, whereas at 10 days sesqui- and diterpenoids reach their highest level.

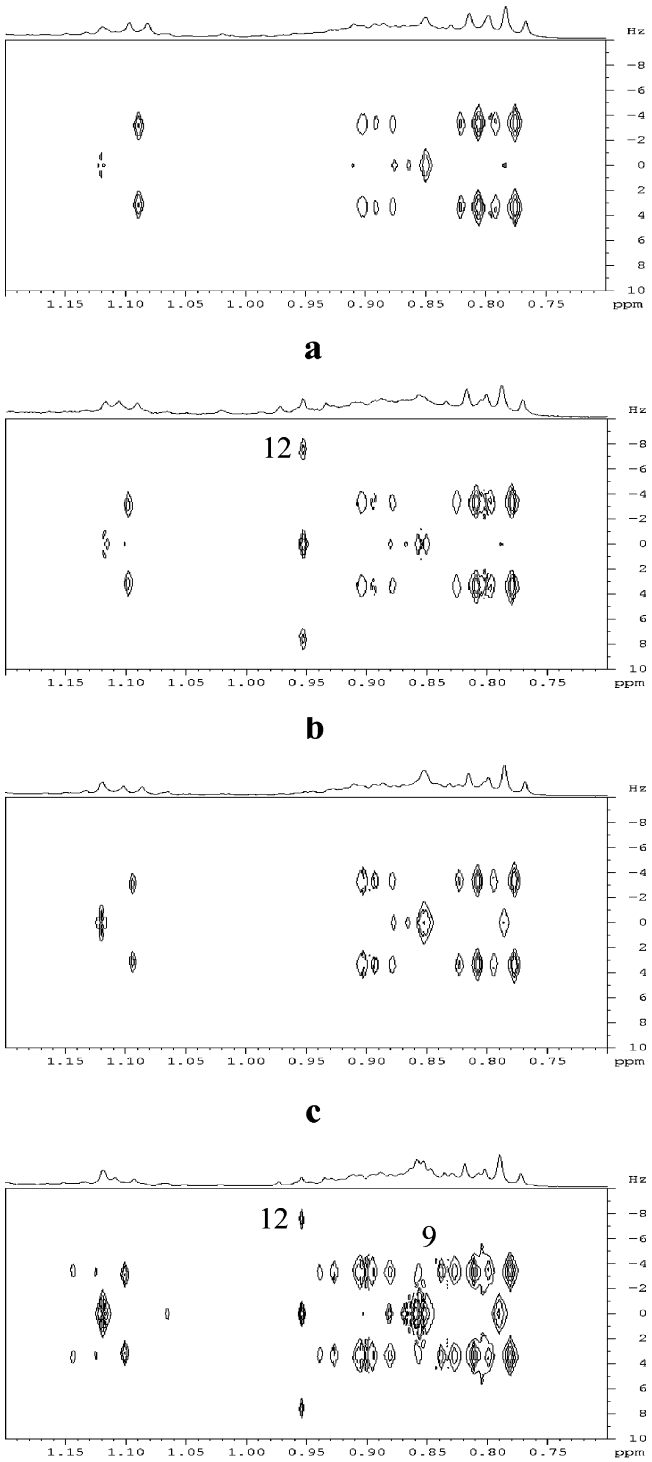

Figure 5. 2-D *J*-resolved NMR spectra of healthy lower leaves (a), TMV locally infected leaves 3 days after inoculation (b), healthy upper leaves (c), and systemic acquired resistance leaves 10 days after inoculation (d) in the range δ 0.5−1.8: (9) capsidiol, (12) α-linolenic acid.

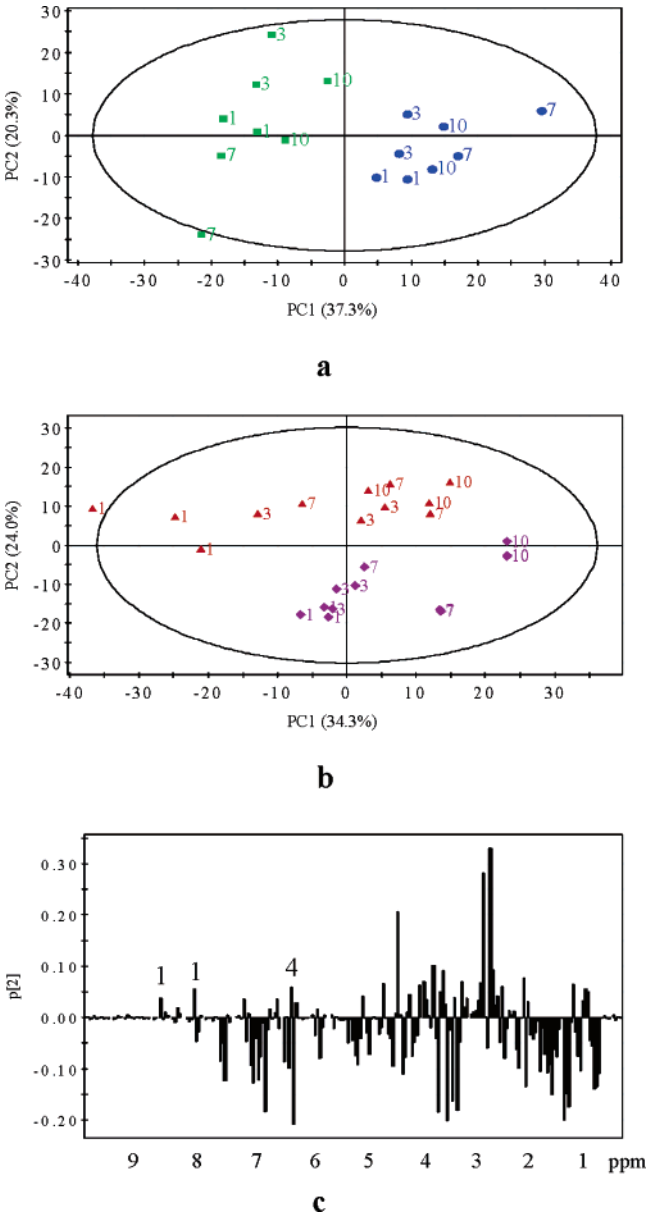

Figure 6. Score plot of principal component analysis of healthy (lower and upper, a) and infected (locally infected and systemic acquired resistant, b) *N. tabacum* leaves by tobacco mosaic virus, and loading plot (PC2) of infected leaves (c): (●) lower leaves of healthy plants, (■) upper leaves of healthy plants, (▲) locally infected leaves of TMV-infected plants, (◆) systemic acquired resistance leaves of TMV-infected plants. (a) Principal component analysis for lower and upper leaves in healthy plants and inoculated and systemic acquired resistance leaves. (b) PCA for lower leaves in healthy plants and inoculated leaves in the infected plants. (c) PCA for upper leaves in healthy plants and systemic acquired resistance leaves in the infected plants. The ellipse represents the Hotelling T2 with 95% confidence in score plots. Numberings on the plots a and b are the number of days after infection. The numerals 1 and 4 on plot c are nicotine and 5-caffeoylquinic acid signals, respectively.

Phenylpropanoid and α-linolenic acid analogue contents in the SAR leaves started to increase seven to 10 days after inoculation, as opposed to the induction at an earlier stage in the locally infected leaves. This observation raises the question whether the phenylpropanoids and α-linolenic acid analogues are transported to SAR leaves from the inoculated site or are part of a defense mechanism stimulated by a signal molecule. To evaluate the differences within the infected plant, a comparison was made of locally infected and SAR leaves in the same plant. From Figure 6 it is clear that PC2 particularly separates these. The main PC2 determining products are nicotine and 5-caffeoyl quinate, which are higher in the locally infected leaves than in the SAR leaves. The trend is opposed of the normal development in the healthy plant.

On the basis of the PCA from analysis of all 1-D and 2-D NMR measurements, a total scheme of the major metabolomic alterations

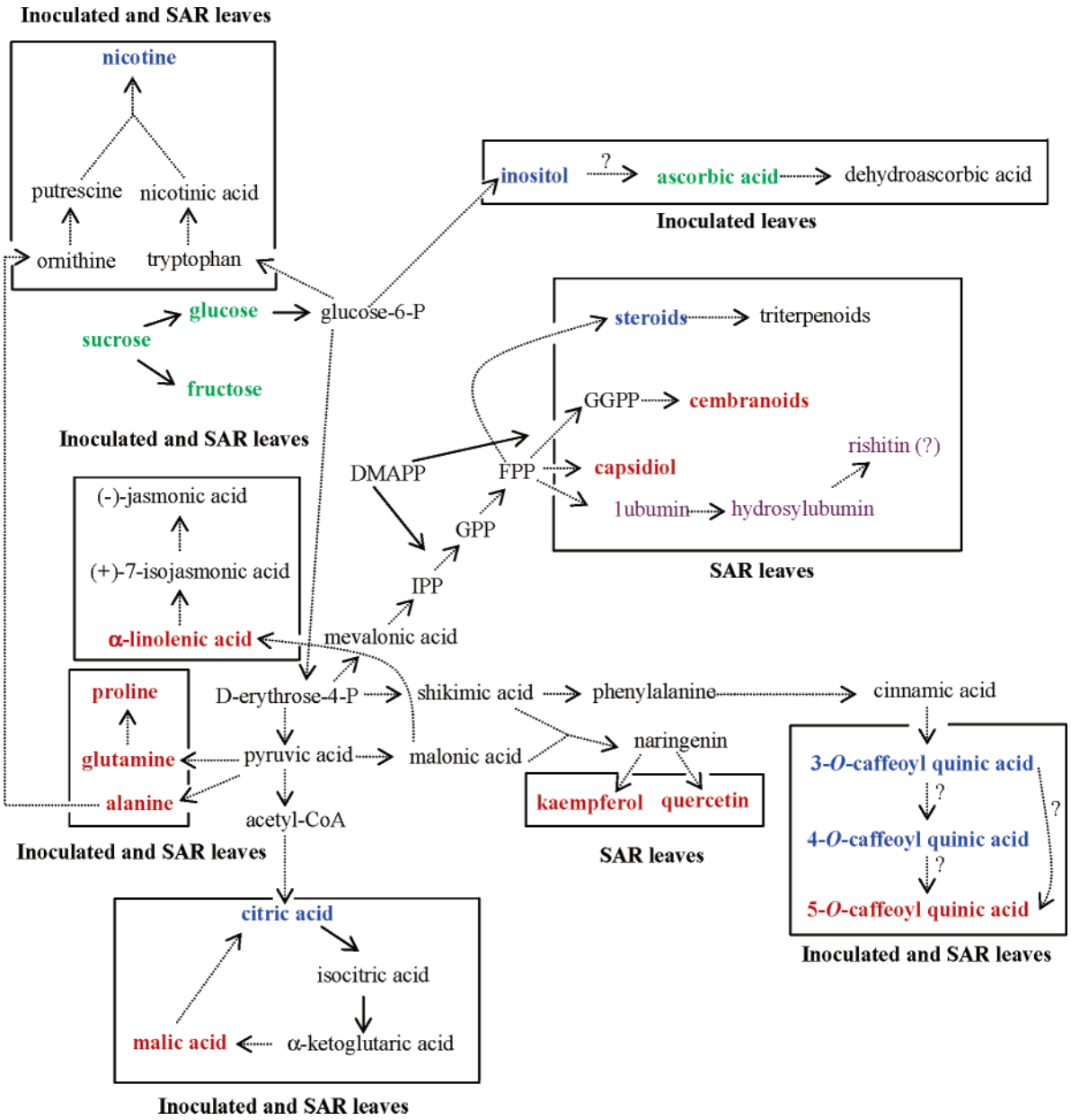

Figure 7. Proposed metabolomic alterations in the *N. tabacum* leaves infected by tobacco mosaic virus: (blue) decreased, (red) increased, (green) transient increased, (purple) previous results from other *N.* species (e.g., *N. undulata*, *N. rustica*, or *N. glutinosa*), (black) based on general plant biosynthesis.

including previous results of sesquiterpenoids[20−22] was prepared (Figure 7). This scheme illustrates clearly the advantage of NMR in metabolomic studies. By a simple extraction a broad variety of primary and secondary compounds can be observed, and conclusions can be drawn about the major changes occurring in the metabolic pathways leading to the various metabolites. Using 1-D ^{1}H NMR spectroscopy in combination with 2-D *J*-resolved spectra and their projection spectra, a macroscopic view of the metabolic changes is obtained. 2-D NMR is a major tool to identify the various metabolites connected with the biological changes. Using this approach several new leads for further studies of tobacco defense mechanisms against TMV were found.

Experimental Section

Plant Material. Twenty-four individual plants of *Nicotiana tabacum* L. were inoculated with TMV three weeks after germination. The TMV inoculation was performed according to the method of Enyedi et al.[23]

Extraction of Plant Material. Each sample was freeze-dried. Then 150 mg of dry material was transferred to a 10 mL centrifuge tube to which 2 mL of 50% MeOH-d_4 in buffer (90 mM KH_2PO_4, apparent pH 7) containing 0.05% TSP (trimethylsilylpropionic acid sodium salt, w/v) was added. The mixture was vortexed at room temperature for 30 s, ultrasonicated for 1 min, and centrifuged at 30000 rpm at 4 °C for 20 min. Then 800 μL of the supernatant was taken for NMR analysis. For the purification of the phenylpropanoid fraction, the freeze-dried plant material (20 g) was extracted with 50% MeOH to afford an initial MeOH extract residue of 2.3 g. An aqueous suspension of this extract was subjected to glass column chromatography over diaion HP-20 resin (40 g, Mitzubishi, Tokyo, Japan) using H_2O and 25% 50%, 75%, and 100% EtOH/H_2O as an eluent. Five hundred milliliter fractions were collected. Of these fractions the 25% EtOH fraction (600 mg) was further fractioned by chromatography with a column of 30 g of Sephadex LH-20 (Pharmacia, Amsterdam, The Netherlands) using 50% MeOH as an eluent to afford 30 fractions (20 mL per each fraction). Using ^{1}H NMR, fractions 10−15 (150 mg) were found to contain the targeted phenylpropanoids.

NMR Analysis. ^{1}H NMR and *J*-resolved spectra were recorded at 25 °C on a 400 MHz Bruker AV-400 spectrometer operating at a proton NMR frequency of 400.13 MHz. MeOH-d_4 was used as the internal lock. Each ^{1}H NMR spectrum consisted of 128 scans requiring 10 min acquisition time with the following parameters: 0.25 Hz/point, pulse

width (PW) = 90° (6.6 μs), and relaxation delay (RD) = 5.0 s. A presaturation sequence was used to suppress the residual H_2O signal with low-power selective irradiation at the H_2O frequency during the recycle delay. FIDs were Fourier transformed with LB = 0.3 Hz, and the spectra were zero-filled to 32K points. The resulting spectra were manually phased and baseline corrected, and calibrated to TSP at 0.0 ppm, using XWIN NMR (version 3.5, Bruker). 2-D *J*-resolved NMR spectra were acquired using 8 scans per 32 increments, which were collected into 16K data points, using spectral widths of 5208 Hz in F2 (chemical shift axis) and 50 Hz in F1 (spin−spin coupling constant axis). A 1.0 s relaxation delay was employed, giving a total acquisition time of 14.52 min. Data sets were zero-filled to 512 points in F1, and both dimensions were multiplied by sine-bell functions (SSB = 0) prior to double complex FT. *J*-resolved spectra tilted by 45° were symmetrized about F1 and then calibrated, using XWIN NMR (version 3.5, Bruker). Data were exported as the 1-D projection (F2 axis) of the 2-D *J*-resolved spectra.

^{1}H−^{1}H COSY, HSQC, and HMBC were measured on a 600 MHz Bruker DMX-600 spectrometer operating at a proton NMR frequency of 600.13 MHz. The COSY spectra were acquired with a 1.0 s relaxation delay, 6361 Hz spectral width in both dimensions. The window function for the COSY spectra was sine-bell (SSB = 0). The HSQC spectra were obtained with a 1.0 s relaxation delay, 6361 Hz spectral width in F2 and 27 164 Hz in F1. Qsine (SSB = 2.0) was used for the window function of HSQC. The HMBC spectra were recorded with the same parameters as the HSQC spectrum except for the 30 183 Hz spectral width in F2. The optimized coupling constants for HSQC and HMBC were 145 and 8 Hz, respectively.

Data Analysis. The ^{1}H NMR and the *J*-resolved projection spectra were automatically reduced to ASCII files using AMIX (v. 3.7, Bruker Biospin). Spectral intensities were scaled to TSP and reduced to integrated regions of equal width (0.04 ppm) corresponding to the region δ −0.40 to 10.00. The region δ 4.7−5.0 was excluded from the analysis because of the residual signal of H_2O. The region of citric acid, malic acid, and succinic acid in δ 2.8−2.5 was bucketed by 0.1 ppm in order to avoid problems due to the dependence of the chemical shifts on the concentration of these compounds. Principle component analyses (PCA) were performed with the SIMCA-P software (v. 10.0, Umetrics, Umeå, Sweden). The Pareto scaling method, which gives each variable a variance numerically equal to its initial standard deviation, was used. Positional matching of *J*-resolved and HSQC spectra was performed with AMIX (v. 3.7, Bruker Biospin).

Acknowledgment. We appreciate the financial support of the Van Leersumfonds (KNAW).

References and Notes

(1) Malamy J.; Carr, J. P.; Klessig, D. F.; Raskin I. *Science* **1990**, *250*, 1002.
(2) Ward, E. R.; Uknes, S. J.; Williams, S. C.; Dincher, S. S.; Wiederhold, D. L.; Alexander, D. C.; Ahl-Goy, P.; Metraux, J. P.; Ryals, J. A. *Plant Cell* **1991**, *3*, 1085.
(3) Nugroho, L. T.; Verberne, M. C.; Verpoorte, R. *Plant Physiol. Biochem.* **2002**, *40*, 755.
(4) Nugroho, L. T.; Peltenburg-Looman, A. M. G.; Verberne, M. C.; Verpoorte, R. *Plant Sci.* **2002**, *162*, 989.
(5) Nugroho, L. T.; Peltenburg-Looman, A. M. G.; De Vos, H.; Verberne, M. C.; Verpoorte, R. *Plant Sci.* **2002**, *162*, 575.
(6) Potts, B. C. M.; Deese, A. J.; Stevens, G. J.; Reily, M. D.; Robertson, D. G.; Theiss, J. *J. Pharm. Biomed. Anal.* **2001**, *26*, 463.
(7) Brindle, J. T.; Antii, H.; Holmes, E.; Tranter, G.; Nicholson, J. K.; Benthell, H. W.; Clarke, S.; Schofield, P. M.; McKilligin, E.; Mosedale, D. E.; Grainger, D. J. *Nat. Med.* **2002**, *8*, 1439.
(8) Holmes, E.; Foxall, P. J.; Nicholson, J. K.; Neild, G. H.; Brown, S. M.; Beddell, C. R.; Sweatman, B. C.; Rahr, E.; Lindon, J. C.; Spraul, M.; Neidig, P. *Anal. Biochem.* **1994**, *220*, 284.
(9) Choi, H.-K. Choi, Y. H.; Verberne, M. C.; Lefeber, A. W. M.; Erkelens, C.; Verpoorte, R. *Phytochemistry* **2004**, *65*, 857.
(10) Viant, M. R. *Biochem. Biophys. Res. Commun.* **2003**, *310*, 943.
(11) Dixon, R. A. *Nature* **2001**, *411*, 843.
(12) Shadle, G. L.; Wesley, S. V.; Korth, K. L.; Chen, F.; Lamb, C.; Dixon, R. A. *Phytochemistry* **2003**, *64*, 153.
(13) Pallas, J. A.; Paiva, N. L.; Lamb, C. J.; Dixon, R. A. *Plant J.* **1996**, *10*, 281.
(14) Sheveleva, E. V.; Marquez, S.; Chmara, W.; Zegeer, A.; Jensen, R. G.; Bohnert, H. J. *Plant Physiol.* **1998**, *117*, 831.
(15) Gawer, M.; Norberg, P.; Chervin, D.; Guern, N.; Yaniv, Z.; Mazliak, P.; Kader, J.-C. *Plant Sci.* **1999**, *141*, 117.
(16) Tan, Z.; Boss, W. F. *Plant Physiol.* **1992**, *100*, 2116.
(17) Staiger, C. J.; Goodbody, K. C.; Hussey, P. J.; Valenta, R.; Drϕbak, B. K.; Lloyd, C. W. *Plant J.* **1993**, *4*, 631.
(18) Yang, W.; Burkhart, W.; Cavallius, J.; Merrick, W. C.; Boss, W. F. *J. Biol. Chem.* **1993**, *268*, 392.
(19) Farmer, E. E.; Ryan, C. A. *Proc. Natl. Acad. Sci. U.S.A.* **1990**, *87*, 7713.
(20) Whitehead, I. M.; Ewing, D. F.; Threlfall, D. R. *Phytochemistry* **1988**, *27*, 1365.
(21) Fuchs, A.; Slobbe, W.; Mol, P. C.; Posthumus, M. A. *Phytochemistry* **1983**, *22*, 1197.
(22) Uegaki, R.; Fujimori, T.; Kubo, S.; Kato, K. *Phytochemistry* **1981**, *20*, 1567.
(23) Enyedi, A. J.; Yalpani, N.; Silverman, P.; Raskin, I. *Cell* **1992**, *70*, 879.

NP050535B